Kinetochore-localized BUB-1/BUB-3 complex promotes anaphase onset in *C. elegans*

Taekyung Kim,[1,2] Mark W. Moyle,[1,2] Pablo Lara-Gonzalez,[1,2] Christian De Groot,[1,2] Karen Oegema,[1,2] and Arshad Desai[1,2]

[1]Ludwig Cancer Research and [2]Department of Cellular and Molecular Medicine, University of California, San Diego, La Jolla, CA 92037

The conserved Bub1/Bub3 complex is recruited to the kinetochore region of mitotic chromosomes, where it initiates spindle checkpoint signaling and promotes chromosome alignment. Here we show that, in contrast to the expectation for a checkpoint pathway component, the BUB-1/BUB-3 complex promotes timely anaphase onset in *Caenorhabditis elegans* embryos. This activity of BUB-1/BUB-3 was independent of spindle checkpoint signaling but required kinetochore localization. BUB-1/BUB-3 inhibition equivalently delayed separase activation and other events occurring during mitotic exit. The anaphase promotion function required BUB-1's kinase domain, but not its kinase activity, and this function was independent of the role of BUB-1/BUB-3 in chromosome alignment. These results reveal an unexpected role for the BUB-1/BUB-3 complex in promoting anaphase onset that is distinct from its well-studied functions in checkpoint signaling and chromosome alignment, and suggest a new mechanism contributing to the coordination of the metaphase-to-anaphase transition.

Introduction

Kinetochores are multiprotein structures assembled on centromeres during mitosis to segregate chromosomes (Cheeseman and Desai, 2008; Santaguida and Musacchio, 2009). Microtubule-generated forces on kinetochores are counteracted by cohesins, which hold sister chromatids together (Onn et al., 2008; Nasmyth and Haering, 2009). Once all sister kinetochores are bioriented, cohesin is proteolytically cleaved by separase to separate sister chromatids. This transition from metaphase to anaphase is controlled by the anaphase-promoting complex/cyclosome (APC/C), a multisubunit E3 ubiquitin ligase (Pines, 2011; Primorac and Musacchio, 2013), and by phosphatases that reverse mitotic phosphorylation events (Sullivan and Morgan, 2007). Significant progress is being made in understanding APC/C mechanism and regulation (Primorac and Musacchio, 2013; Chang and Barford, 2014) and the contributions of phosphatases during mitotic exit (Sullivan and Morgan, 2007; Bollen et al., 2009; Hunt, 2013; Wieser and Pines, 2015), but how anaphase onset is precisely coordinated with chromosome alignment remains an important question.

Multiple mechanisms control APC/C activity. Increasing Cdk1 activity is proposed to trigger cyclin degradation (Murray and Kirschner, 1989; Félix et al., 1990). Consistent with this, Cdk1 phosphorylation of APC/C subunits promotes interaction with its coactivator Cdc20 (Peters et al., 1996; Kramer et al., 2000; Kraft et al., 2003). APC/C activation is opposed by the spindle assembly checkpoint, which inhibits the ability of Cdc20 to fully activate APC/C when unattached kinetochores are present (Musacchio and Salmon, 2007; Lara-Gonzalez et al., 2012). After attachment, checkpoint silencing enables progression into anaphase (Sacristan and Kops, 2014). Phosphorylation of Cdc20 by Cdk1 inhibits its ability to bind and activate APC/C, which suggests that reversal of these phosphorylation events is important for anaphase onset (Kramer et al., 2000; Yudkovsky et al., 2000; Labit et al., 2012). Phosphatase activities are also important for reversing Cdk1 phosphorylation but their control is less well understood. A PP2A regulatory pathway involving Greatwall kinase and its substrates endosulphine A and Arpp19, both PP2A inhibitors, has been implicated in both entry and exit from mitosis (Gharbi-Ayachi et al., 2010; Mochida et al., 2010). A phosphatase relay mechanism involving PP1 and PP2a that is important for mitotic progression has also been recently described (Grallert et al., 2015).

Correspondence to Arshad Desai: abdesai@ucsd.edu

Abbreviations used in this paper: APC/C, anaphase-promoting complex/cyclosome; CI, confidence interval; dsRNA, double-stranded RNA; NEBD, nuclear envelope breakdown.

The Rockefeller University Press $30.00
J. Cell Biol. Vol. 209 No. 4 507–517
www.jcb.org/cgi/doi/10.1083/jcb.201412035

Here, we uncover a new role for two conserved checkpoint components, Bub1 kinase and its binding partner the WD40-fold protein Bub3 (Hoyt et al., 1991; Roberts et al., 1994; Taylor et al., 1998), in promoting anaphase onset. The Bub1/Bub3 complex is recruited to kinetochores by binding to phosphorylated repetitive motifs in the N terminus of Knl1, a scaffold component of the Knl1/Mis12 complex/Ndc80 complex (KMN) network (London et al., 2012; Yamagishi et al., 2012; Shepperd et al., 2012; Primorac et al., 2013). Kinetochore-localized Bub1/Bub3 recruits other spindle checkpoint components including Mad1/Mad2 and BubR1 (Sharp-Baker and Chen, 2001; Gillett et al., 2004; Johnson et al., 2004; Vanoosthuyse et al., 2004; London and Biggins, 2014; Moyle et al., 2014). Bub1 has also been proposed to inhibit the APC/C by phosphorylation of its activator Cdc20 (Tang et al., 2004).

In addition to its role in the checkpoint, the Bub1/Bub3 complex contributes to chromosome alignment and segregation (Warren et al., 2002; Vanoosthuyse et al., 2004; Meraldi and Sorger, 2005; Fernius and Hardwick, 2007; Klebig et al., 2009). Bub1 phosphorylates histone H2A to create a binding site for Shugoshin, which recruits protein phosphatase 2A (PP2A) and Aurora B kinase to the inner centromere (Kawashima et al., 2010; Yamagishi et al., 2010). In vertebrates, Bub1 also recruits BubR1, CENP-E, CENP-F, and dynein, which contribute to proper chromosome alignment (Sharp-Baker and Chen, 2001; Johnson et al., 2004; Klebig et al., 2009).

Here we show that, in the early *Caenorhabditis elegans* embryo, kinetochore-localized BUB-1/BUB-3 promotes anaphase onset, and that this function is independent of its roles in spindle checkpoint signaling and chromosome alignment. These results identify a new function embedded in the Bub1/Bub3 complex and suggest a potential mechanism contributing to the coordination of chromosome alignment and anaphase onset.

Results and discussion

BUB-1/BUB-3 removal delays anaphase onset independently of checkpoint signaling

Analysis of one-cell *C. elegans* embryos expressing GFP fusions to label chromosomes and spindle poles revealed that depletion of BUB-1 increased the time from nuclear envelope breakdown (NEBD) to anaphase onset by ∼50% (Fig. 1, A and C). This was surprising because BUB-1 is required for the spindle checkpoint, which restrains anaphase onset; thus, one would not expect removal of BUB-1 to delay anaphase onset. As BUB-1 also functions in chromosome alignment (Fig. S1 A), one possible explanation is that partial penetrance of the BUB-1 depletion resulted in improperly attached chromosomes with sufficient residual BUB-1 to generate a spindle checkpoint signal and delay anaphase onset, a scenario reported in multiple mammalian Bub1 RNAi experiments (Johnson et al., 2004; Meraldi and Sorger, 2005; Klebig et al., 2009). As BUB-1 was >94% depleted (Fig. 1 B), this seemed unlikely. However, to test this further, we co-depleted BUB-1 and MAD-2 (also known as MDF-2). MAD-2 depletion abrogates checkpoint signaling in *C. elegans* embryos (Essex et al., 2009; Espeut et al., 2012) but did not suppress the anaphase onset delay resulting from BUB-1 depletion (Fig. 1, A and C). Thus, the observed delay in anaphase onset is not due to residual BUB-1 generating a checkpoint signal.

BUB-1 associates with BUB-3 via a conserved binding motif that follows its N-terminal TPR domain (Taylor et al., 1998; Wang et al., 2001; Larsen et al., 2007). The BUB-1/BUB-3 complex docks onto phosphorylated motifs in the KNL-1 N terminus (Primorac et al., 2013). A BUB-3 deletion mutant (*bub-3(ok3437)*, referred to as *bub-3Δ*; Fig. S1 B), exhibited a comparable NEBD–anaphase onset delay to that resulting from BUB-1 depletion (Fig. 1 C and Fig. S1 C). BUB-1 kinetochore localization (Fig. 1 D), as well as its overall protein levels (Fig. S1 D), was significantly reduced in *bub-3Δ*. Conversely, BUB-3 kinetochore localization was significantly disrupted by BUB-1 depletion (Fig. 1 D), albeit without a reduction in BUB-3 protein levels (Fig. S1 E). Thus, depletion of BUB-1 should be considered as perturbing the BUB-1/BUB-3 complex.

BUB-1 depletion had no effect on interphase duration, measured as the interval between anaphase onset in the one-cell embryo and NEBD of the AB cell in the two-cell embryo (Fig. 1 E); in contrast, the NEBD–anaphase onset interval was delayed in the AB cell (Fig. 1 E), indicating that promotion of timely anaphase onset by the BUB-1/BUB-3 complex is not restricted to the first embryonic division. Thus, inhibition of the BUB-1/BUB-3 complex delays anaphase onset, and this delay is independent of spindle checkpoint signaling.

BUB-1/BUB-3 complex localization to kinetochores is required for promotion of anaphase onset

A significant pool of BUB-1/BUB-3 is retained on kinetochores after bipolar attachment of chromosomes (Fig. 2 A; Jablonski et al., 1998; Taylor et al., 2001; Gillett et al., 2004). To test if the ability of BUB-1/BUB-3 to promote anaphase required localization to kinetochores, we analyzed deletion mutants in the phosphorylation-dependent BUB-1/BUB-3 docking motifs in the KNL-1 N terminus (Fig. 2 B). The largest KNL-1 deletion tested (Δ85–505) is expressed, localizes to kinetochores but prevents BUB-1 kinetochore localization without affecting BUB-1 protein levels (Fig. 2, C and D; Moyle et al., 2014), and is checkpoint signaling–defective (Fig. S2 A). KNL-1(Δ85–505) delayed anaphase onset to a similar extent as BUB-1 depletion (Fig. 2, E and F). Two smaller nonoverlapping deletions within this region (Δ85–290 and Δ291–505) both localized to kinetochores but reduced BUB-1 kinetochore localization by approximately half (Fig. 2 C; metaphase kinetochore BUB-1::GFP fluorescence intensity of 56 ± 17%; $n = 11$ for Δ85–290 and 40 ± 16%; $n = 16$ for Δ291–505, relative to wild-type [WT] KNL-1; data from Moyle et al., 2014) and caused an intermediate delay in anaphase onset (Fig. 2, E and F). Thus, kinetochore localization is required for the BUB-1/BUB-3 complex to promote anaphase onset, and the amount of kinetochore-localized BUB-1 influences the magnitude of the NEBD–anaphase onset interval.

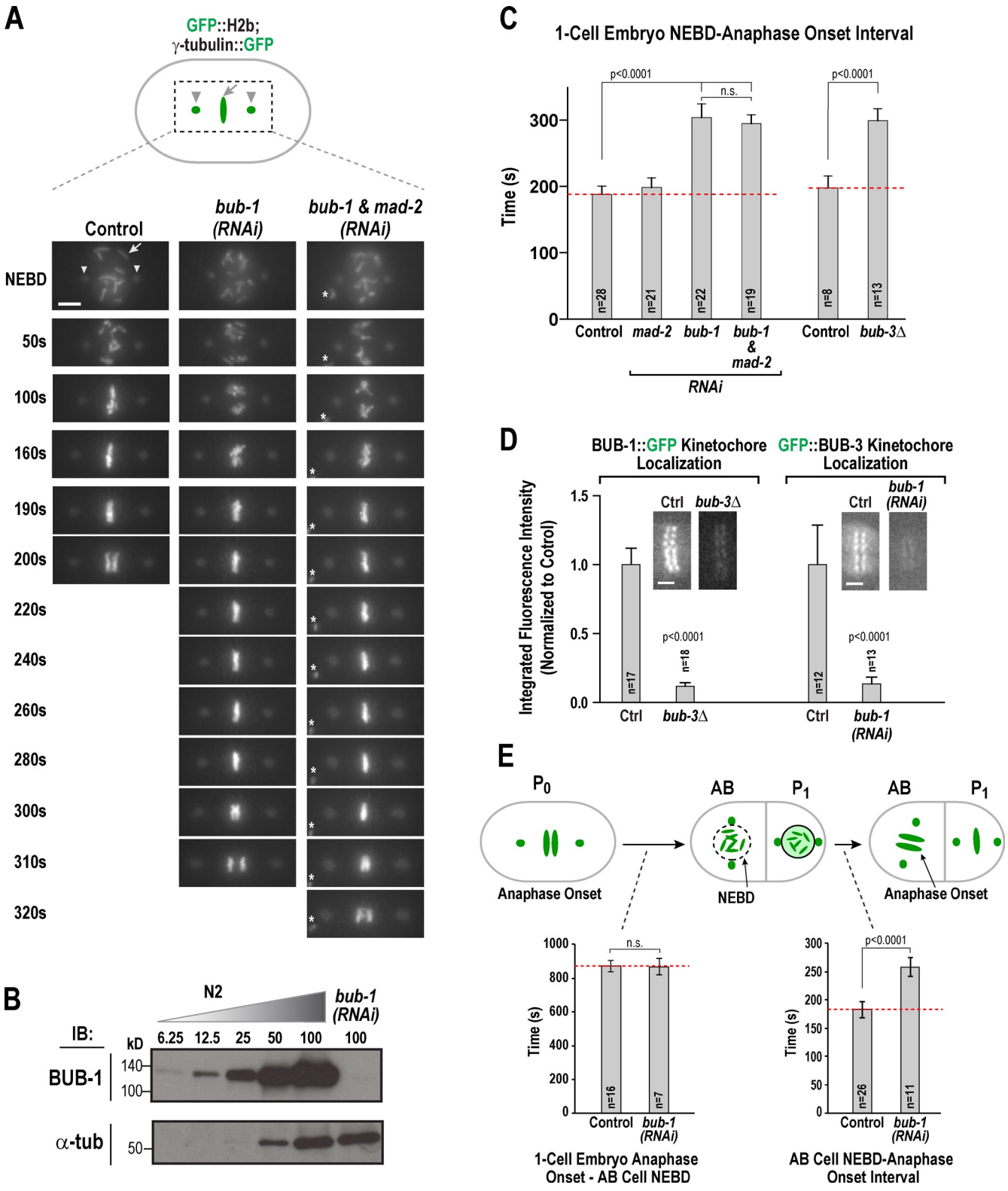

Figure 1. **BUB-1 depletion delays anaphase onset independently of checkpoint signaling.** (A) Images from time-lapse movies of one-cell *C. elegans* embryos expressing GFP::H2b (arrow) and γ-tubulin::GFP (arrowheads) for the indicated conditions. Time is given in seconds after NEBD. The asterisks mark extra chromatin present due to defective meiotic segregation. Bar, 5 μm. (B) Immunoblot of *bub-1(RNAi)* worms next to a dilution of control N2 worms. Numbers indicate the amount loaded relative to the 100% lanes. α-Tubulin is a loading control. (C) Plot of mean NEBD–anaphase onset intervals for the indicated conditions in one-cell embryos. Error bars indicate SD; red broken lines are control values; *n* is the number of embryos. (D) BUB-1 and BUB-3 kinetochore localization in *bub-3Δ* (left) and *bub-1(RNAi)* (right), respectively; *n* is the number of embryos. The mean integrated fluorescence intensity at kinetochores is plotted; error bars indicate the 95% confidence interval (CI). Bars, 2 μm. (E) Schematic indicates the time intervals measured and plotted below. Error bars indicate SD; red broken lines are control values; *n* is the number of embryos.

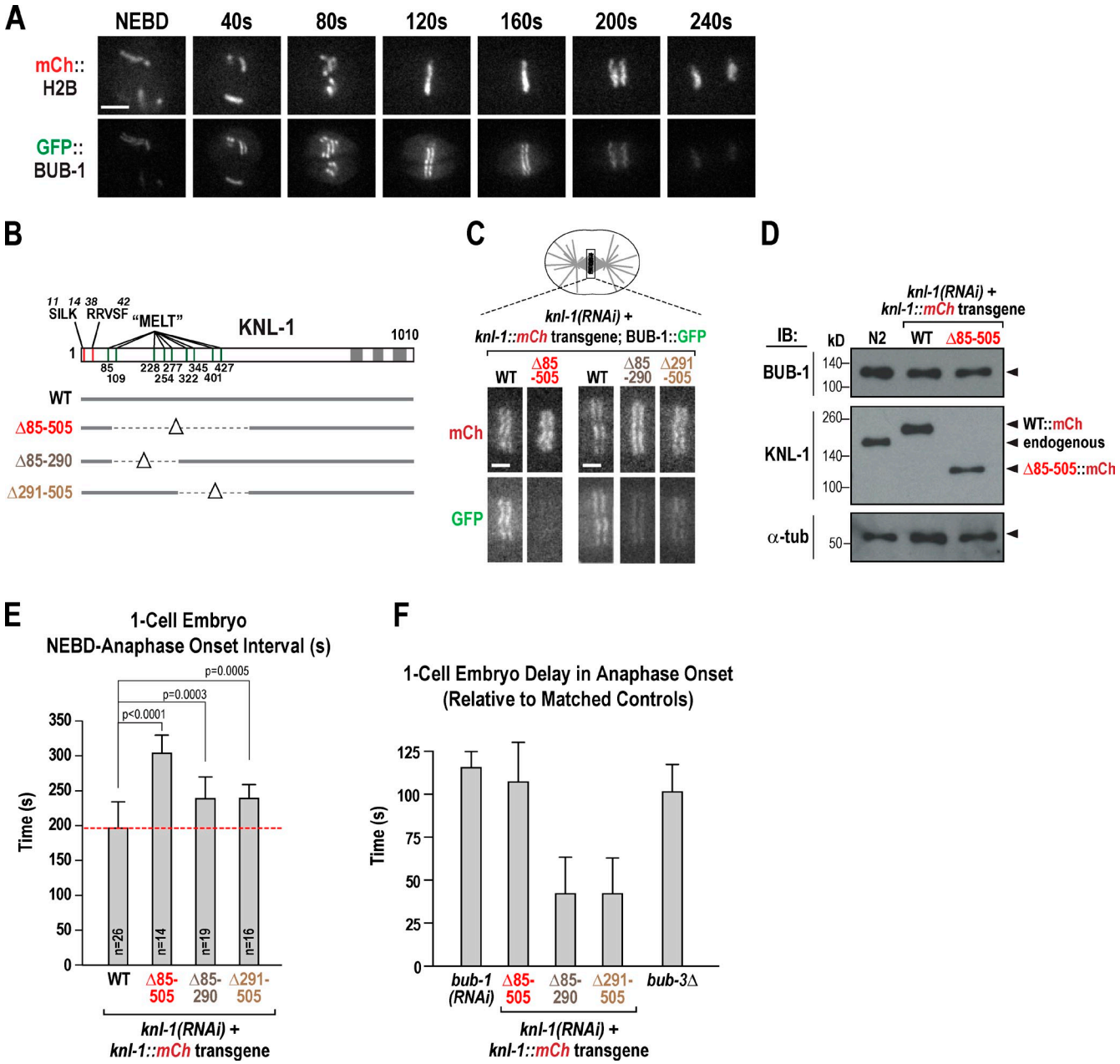

Figure 2. **Kinetochore Localization of BUB-1 is required to promote anaphase onset.** (A) Images from a time-lapse sequence of a one-cell embryo expressing mCh::H2b and GFP::BUB-1. Time is given in seconds after NEBD. Bar, 5 µm. (B) Schematic of features of the KNL-1 N terminus. The deletions analyzed are depicted below. (C) Representative images of BUB-1::GFP localization in the presence of indicated *knl-1* transgenes, after depletion of endogenous KNL-1. Bars, 2 µm. (D) Immunoblots of BUB-1, KNL-1, and α-tubulin, which serves as a loading control, for the indicated conditions. As part of the antigen used to generate the KNL-1 antibody (aa 8–256; Desai et al., 2003) is deleted in the Δ85–505 mutant, the band intensities of WT and Δ85–505 KNL-1 cannot be compared. (E) Plot of mean NEBD–anaphase onset intervals for the indicated conditions in one-cell embryos. Error bars indicate SD; red broken line is the control value; *n* is the number of embryos. (F) Plot of the mean delay in anaphase onset for the indicated conditions, generated by subtracting matched mean control values and propagating errors. Error bars indicate the 95% CI. KNL-1 mutants and their matched control (WT) values are from D; *bub-1(RNAi)*, *bub-3Δ* and their matched control values are from Fig. 1 C.

BUB-1 depletion delays separase activation and other mitotic exit events

BUB-1/BUB-3 may promote anaphase onset by promoting APC/C activation or contributing to a pathway (e.g., activation of Cdk1-countering phosphatases) that functions in parallel to APC/C. While GFP fusions with Cyclin B (CYB-1; Liu et al., 2004) and Securin (IFY-1; Wang et al., 2013) enable monitoring of APC/C activation at meiosis I anaphase in *C. elegans*, GFP signal for these fusions is not detected in early embryos (Liu et al., 2004; Wang et al., 2013; unpublished data), likely because the ∼20-min interval between meiosis II anaphase and NEBD of the first embryonic mitosis (Portier et al., 2007) is too short for GFP maturation at 20°C. This technical issue prevented us from directly monitoring APC/C activity to test if kinetochore-localized BUB-1/BUB-3 controls the timing of its activation. However, we engineered a sensor for activation of separase, the protease

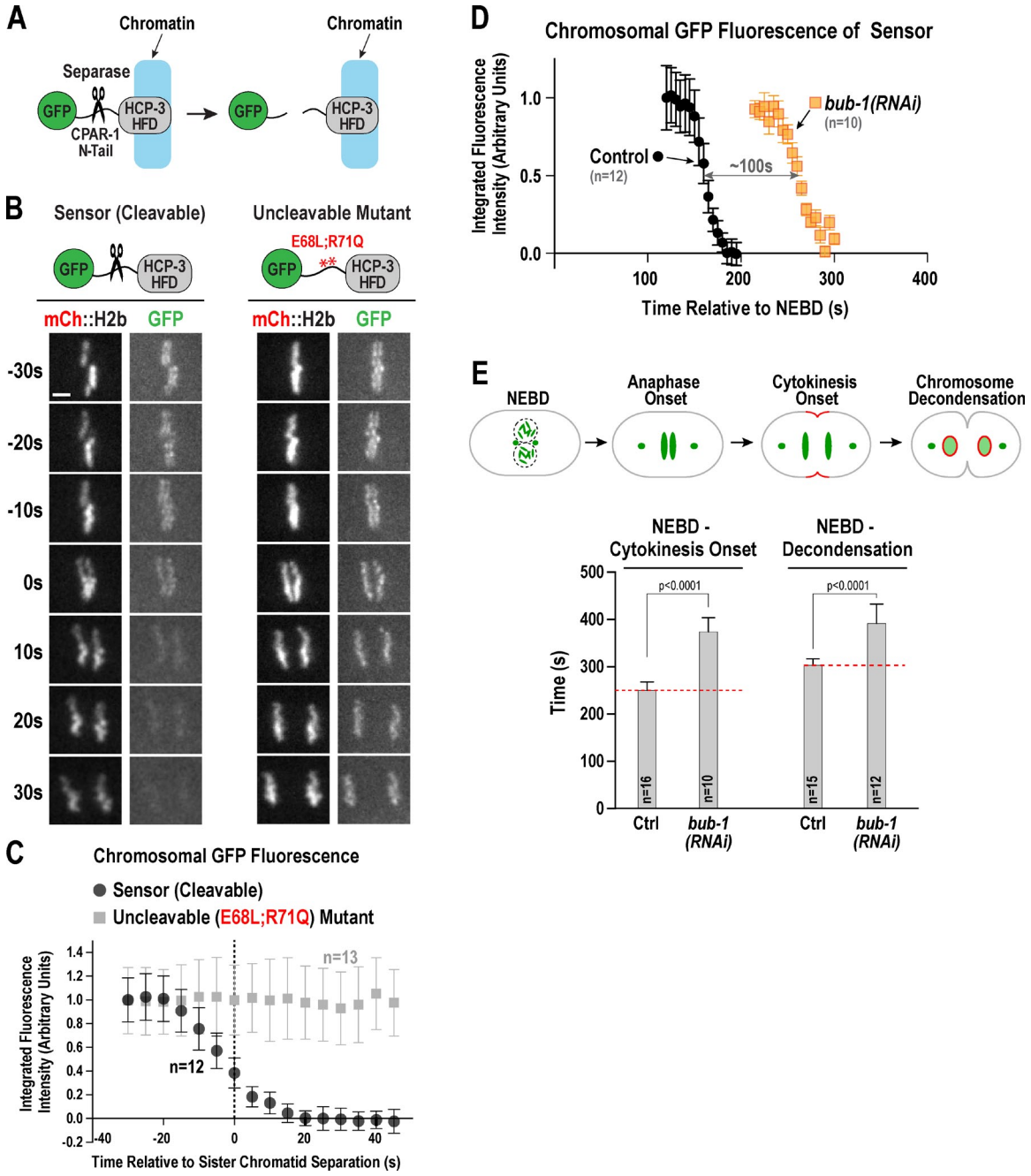

Figure 3. **BUB-1 depletion delays separase activation and other mitotic exit events.** (A) Schematic of sensor used to monitor separase activation in one-cell embryos. (B) Images from time-lapse sequences of strains coexpressing mCh::H2b and either the separase sensor or an uncleavable mutant. GFP imaging at 5-s intervals was initiated ∼50–80 s before anaphase onset; mCherry imaging was initiated earlier to score NEBD. Bar, 2 µm. (C) Plot of mean chromosomal GFP fluorescence for the separase sensor and the uncleavable mutant, relative to sister separation onset. *n* is the number of embryos. Error bars indicate the 95% CI. (D) Plot of mean chromosomal GFP fluorescence of the separase sensor over time, for the indicated conditions. Error bars indicate the 95% CI. (E) Schematic (top) and mean intervals from NEBD (bottom) of other mitotic exit events scored in time-lapse sequences. *n* is the number of embryos analyzed. Error bars indicate SD; red broken lines are control values.

that acts downstream of APC/C activation to cleave cohesin and separate sister chromatids (Uhlmann et al., 2000), based on our identification of a separase cleavage site in the N-tail of the CENP-A–related protein CPAR-1 (Monen et al., 2015). To create a mitotic separase sensor, we fused GFP to the N terminus of a chimeric protein in which the CPAR-1 N-tail was placed in front of the histone fold domain of the major *C. elegans* CENP-A–related protein HCP-3 (HCP-3 HFD; Fig. 3 A). GFP signal of this sensor was observed on metaphase chromosomes but was progressively lost starting 15 s before visible chromatid separation (Fig. 3, A–C). Mutation of two key residues in the predicted cleavage motif (Sullivan et al., 2004) abrogated the signal loss of the sensor (Fig. 3, B and C), confirming that separase cleavage liberated GFP from chromatin. Expression of the sensor did not affect NEBD–anaphase onset interval or embryo production/viability (Fig. S2, B and C).

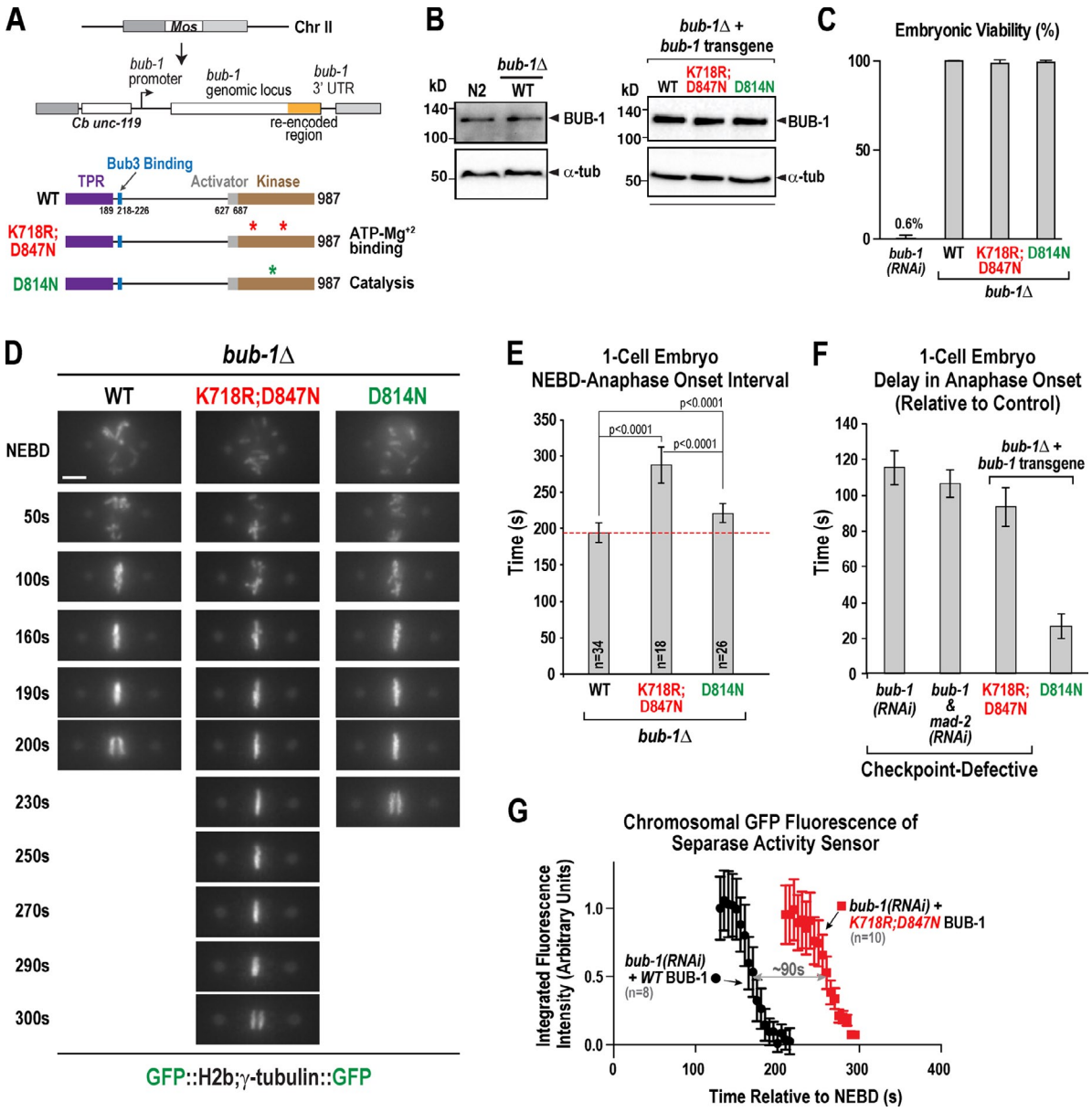

Figure 4. **Mutations in the BUB-1 kinase domain delay anaphase onset to nearly the same extent as BUB-1 depletion.** (A) Schematic of RNAi-resistant *bub-1* transgene and three transgene-encoded variants. (B) BUB-1 immunoblots of the indicated conditions; α-tubulin is a loading control. (C) Embryo viability analysis for the indicated strains and conditions. Error bars indicate the SD of individual worm progeny viability. (D) Images from representative time-lapse sequences as in Fig. 1 A. Bar, 5 µm. (E) Plot of mean NEBD–anaphase onset intervals for the indicated conditions. Error bars indicate SD; the red broken line is the control value; *n* is the number of embryos. (F) Plot of the mean delay in anaphase onset for the indicated conditions, generated by subtracting the matched control values and propagating errors. Error bars indicate the 95% CI. *bub-1(RNAi)* and *bub1&mad-2(RNAi)* values are from Fig. 1 C; other data are from E. (G) Plot of mean chromosomal GFP fluorescence of the separase sensor, for the indicated conditions. Error bars indicate the 95% CI.

Analysis of sensor-expressing embryos revealed that separase activation was delayed by BUB-1 depletion to the same extent as anaphase onset (Fig. 3 D). Once initiated, the kinetics of sensor chromosomal signal loss was not significantly different between the control and the BUB-1 depletion (Fig. 3 D). Thus, kinetochore-localized BUB-1/BUB-3 controls the timing of separase activation relative to NEBD. To determine if the delay induced by BUB-1 depletion was limited to control of separase or represented a general delay in mitotic exit, we examined the timing of two other events that follow sister chromatid separation: cytokinesis onset and chromosome decondensation (Fig. 3 E). Both were delayed in the BUB-1 depletion relative to NEBD (Fig. 3 E), indicating that kinetochore-localized BUB-1/BUB-3 does not act solely to control separase activation but instead functions in a pathway that is broadly relevant for triggering mitotic exit.

Anaphase onset promotion requires the BUB-1 kinase domain but is independent of its kinase activity

To identify features of BUB-1/BUB-3 required to promote anaphase onset, we focused on BUB-1, using single-copy RNAi-resistant transgenes (Fig. 4 A; Moyle et al., 2014). Both untagged

(Fig. 4 C) and mCherry-tagged (not depicted) *bub-1* transgenes fully rescued the 100% penetrant lethality of the *bub-1(ok3383)* mutant (Fig. S3 A; referred to as *bub-1Δ*). However, the C-terminal mCherry-tagged BUB-1 led to a modest increase in the NEBD–anaphase onset interval (Fig. S3 B), which suggests that the C-terminal part of BUB-1, which harbors its kinase domain, may be important for anaphase promotion. Deletion of the kinase domain led to a delay equivalent to that observed for BUB-1 depletion (Fig. S3 B), leading us to characterize mutations in the kinase domain (Fig. 4 A; Moyle et al., 2014). The K718R;D847N mutant, which abrogates kinase activity by altering residues involved in ATP and magnesium binding, fails to localize MAD-1 to kinetochores and is checkpoint-defective; in contrast, the D814N mutant, which abrogates kinase activity by mutating the catalytic aspartate of the "HxD" motif, recruits MAD-1 and supports checkpoint signaling (Moyle et al., 2014). Both mutants were expressed equivalently to WT BUB-1 in a *bub-1*Δ background (Fig. 4 B) and rescued the lethality of *bub-1*Δ (Fig. 4 C; Moyle et al., 2014); mCherry-tagged versions localized normally to kinetochores (Fig. S3 C). Whereas the WT *bub-1* transgene restored the NEBD–anaphase onset interval to that in controls (Fig. 4, D and E; compare to Fig. 1, A and C), the D814N mutant led to a mild extension of the NEBD–anaphase onset interval (Fig. 4, D–F), and the K718R;D847N mutant exhibited delays in anaphase onset, separase activation, cytokinesis onset, and chromosome decondensation comparable to those resulting from BUB-1 depletion (Fig. 4, D–G; and Fig. S3 D). We conclude that the anaphase promotion function of BUB-1/BUB-3, while largely independent of BUB-1 kinase activity, is dependent on a properly structured BUB-1 kinase domain.

The anaphase onset promotion function of the BUB-1/BUB-3 complex is independent of its role in chromosome alignment

Bub1 kinase activity is important for the recruitment of Shugoshin family proteins via histone H2a phosphorylation (Kawashima et al., 2010; Ricke et al., 2012). However, neither depletion nor mutation of SGO-1, the only *C. elegans* member of the Shugoshin protein family, resulted in a NEBD–anaphase onset delay (Figs. 5 A and S3, E–G). Together with the mild effect of the D814N mutant (Fig. 4, D–F), this result suggests that the promotion of anaphase onset by the BUB-1/BUB-3 complex is independent of the BUB-1–phosphoH2a–Shugoshin pathway.

BUB-1 depletion or blocking BUB-1/BUB-3 kinetochore targeting using Δ85-505 KNL-1 led to significant chromosome segregation errors and 100% embryonic lethality; in contrast, no segregation errors were observed in the K718R;D847N mutant, which exhibited normal embryonic viability in the *bub-1Δ* background (Figs. 4 C and 5 B). This conclusion was further supported by localization analysis of HCP-1—one of two functionally redundant *C. elegans* proteins with weak similarity to CENP-F (Moore et al., 1999; Cheeseman et al., 2005). Consistent with prior work (Encalada et al., 2005), HCP-1 was largely delocalized from kinetochores after BUB-1 depletion; in contrast, HCP-1 was normally localized in the K718R;D847N mutant (Figs. 5 C and S3 H). Load-bearing kinetochore–microtubule attachments were also normal in the K718R;D847N mutant. In the one-cell embryo, quantitative analysis of spindle elongation functions as a measure for the formation of load-bearing kinetochore–microtubule attachments, as the cortex generates pulling forces on astral microtubules that are resisted by kinetochore–microtubule attachments in the spindle (Oegema et al., 2001). Tracking spindle pole separation after NEBD revealed delayed load-bearing attachment formation after BUB-1 depletion (Fig. 5 D, left; the delay is evident in the "bump," which indicates premature separation of the spindle poles followed by recovery to control metaphase spindle length), a nearly identical profile was observed in the Δ85-505 KNL-1 mutant that prevents BUB-1/BUB-3 kinetochore recruitment (Fig. 5 D, left). In contrast, the K718R;D847N mutant did not delay attachment formation; instead, there was an extended plateau at metaphase spindle length (Fig. 5 D, right). Thus, K718R;D847N BUB-1, while delaying anaphase onset to nearly the same extent as BUB-1 depletion, does not exhibit the chromosome segregation defects observed after BUB-1 depletion.

Conclusion

Here we describe a new function for kinetochore-localized BUB-1/BUB-3 complex in promoting anaphase onset, which adds to its known roles in checkpoint signaling and chromosome alignment. The conclusion that this new function is independent of checkpoint signaling was supported by four perturbations that inhibit checkpoint signaling: co-depletion of MAD-2, deletion of *bub-3*, removal of the docking site on kinetochores for BUB-1/BUB-3, and the K718R;D847N mutant in the BUB-1 kinase domain. Comparison of BUB-1 kinase active site mutants revealed that the anaphase promotion function resides in the kinase domain but is largely independent of kinase activity. Perturbation of BUB-1/BUB-3 delays but does not block anaphase onset, indicating that BUB-1/BUB-3's anaphase promotion activity functions in parallel to other mechanisms triggering anaphase onset. These parallel mechanisms likely involve many complex phosphorylation events on APC/C, primarily dependent on Cdk1 (Fig. 5 E; Kraft et al., 2003; Labit et al., 2012).

A role for BUB-1/BUB-3 in promoting anaphase appears counterintuitive, given the long-standing focus on BUB-1/BUB-3 as the kinetochore scaffold for the checkpoint signal that inhibits anaphase onset. We speculate that conversion of a key kinetochore-localized negative regulator of anaphase into a positive promoter once necessary conditions, e.g., proper kinetochore-microtubule attachment, have been met, could aid coupling completion of chromosome alignment to activation of separase and sister separation (Fig. 5 E). Our inability to monitor APC/C activation leaves open the question as to the mechanism upstream of separase activation in which BUB-1/BUB-3 acts to promote anaphase onset. An appealing possibility is that kinetochore-localized BUB-1/BUB-3 promotes APC/C activation (Fig. 5 E, top right). Bub1 is known to bind the APC/C activator Cdc20, and, while prior work has focused on the significance of this interaction in checkpoint signaling and Bub1 degradation (Tang et al., 2004; Kang et al., 2008; Di Fiore et al., 2015), our results raise the possibility that Cdc20 binding could contribute positively to APC/C activation. An alternative possibility is that BUB-1/BUB-3 functions in a pathway, such

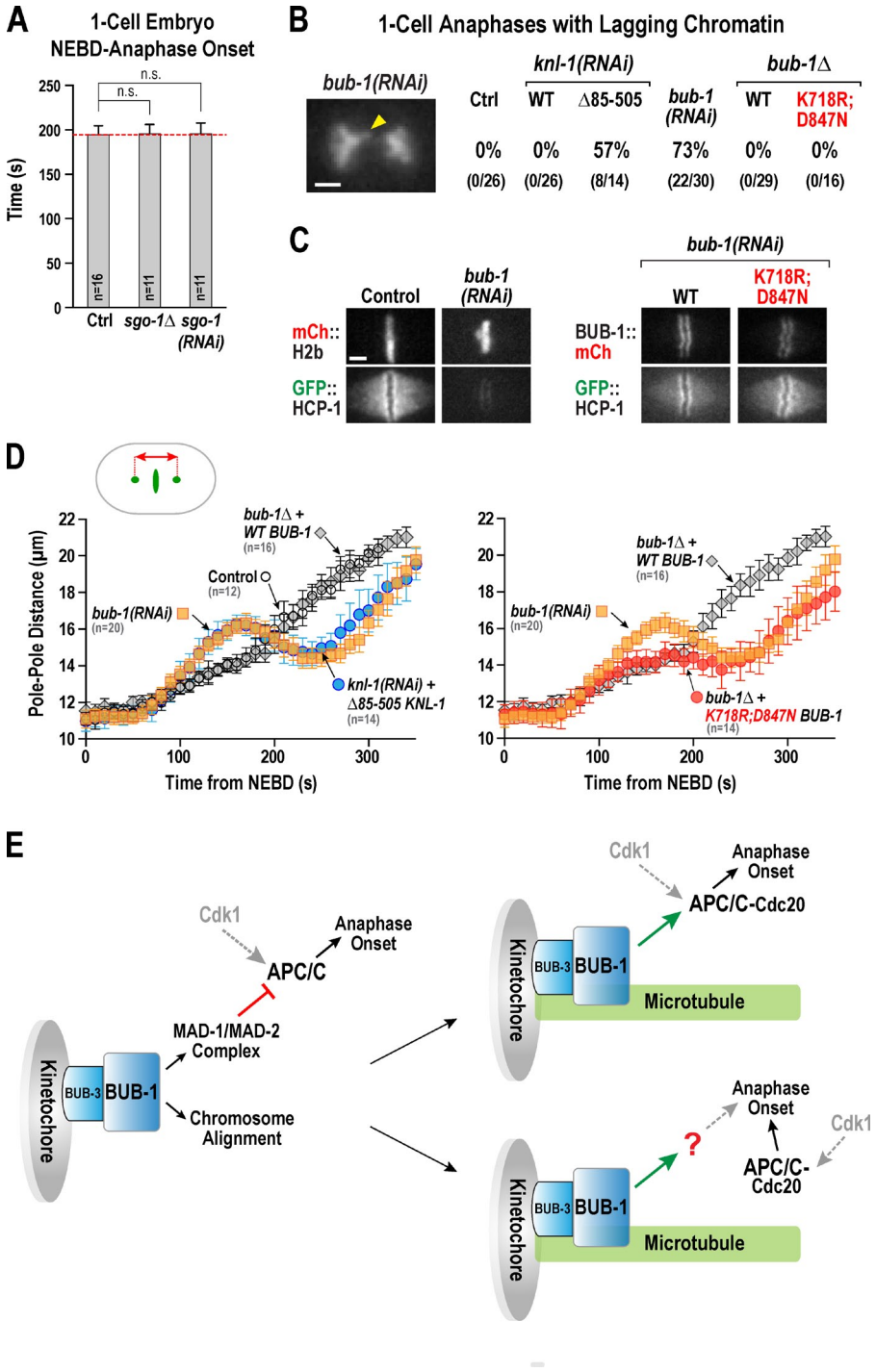

Figure 5. **The anaphase promotion function of BUB-1 can be uncoupled from its role in chromosome alignment.** (A) Plot of mean NEBD–anaphase onset intervals for the indicated conditions in one-cell embryos. Error bars indicate SD; the red broken line is the control value; *n* is the number of embryos. (B) Frequency of anaphase lagging chromatin (yellow arrowhead in the example image on the left) in one-cell embryos for the indicated conditions. Bar, 2 µm. (C) Images of metaphase one-cell embryos expressing GFP::HCP-1. Endogenous HCP-1 and HCP-2 were depleted by RNAi to enhance the GFP::HCP-1 signal. Bar, 2 µm. (D) Spindle pole separation profiles over time (relative to NEBD) for the indicated conditions. *n* is the number of embryos analyzed. Error bars indicate the 95% CI. In the left plot, the control (open circles) and *bub-1Δ+WT* BUB-1 (gray diamond) profiles are largely overlapping, as are the profiles of *bub-1(RNAi)* (orange squares) and *knl-1(RNAi)+Δ85-505* KNL-1 (blue circles). (E) Speculative model for coordination of the metaphase-to-anaphase transition. BUB-1/BUB-3 controls checkpoint signaling at unattached kinetochores, which restrains APC/C activity (left); in addition, BUB-1/BUB-3 promotes kinetochore-microtubule attachment and chromosome alignment. Once chromosomes are aligned and the checkpoint is satisfied, BUB-1 promotes anaphase onset either via APC/C (top right) or via a parallel pathway (bottom right).

as activation of a phosphatase, that acts in parallel with APC/C to promote anaphase onset (Fig. 5 E, bottom right). Future work is needed to distinguish between these possibilities.

Materials and methods

C. elegans strains

C. elegans strains used in this study are listed in Table S1 and were maintained at 20°C. RNAi-resistant *bub-1* and *knl-1* transgenes, together with information on their recoded regions, have been described previously (Espeut et al., 2012; Moyle et al., 2014). For the RNAi-resistant *bub-1* transgenes, the short (44-bp) intron 5 was deleted and 122 bp of exon 5 and all of exon 6 were recoded. For RNAi-resistant *knl-1* transgenes, exon 4 was recoded. The *bub-1* transgenes were transferred into pCFJ151 (Frøkjær-Jensen et al., 2008), a vector used to generate insertion at the *attTi5605* locus on Chr II, before injection into strain EG4322. The presence of transgenes and of engineered mutations was confirmed by PCR and sequencing. For the separase sensor, the CPAR-1 N-tail (2–159 aa) and HCP-3 histone-fold domain (187–288 aa) were amplified from genomic DNA and fused together. GFP was inserted after the start codon and followed by a GGRAGSGGRAGSGGRAGS linker, inserted into pCFJ151, and injected into the strain EG6429. GFP::H2b; γ-tubulin::GFP, mCherry::H2b, BUB-1::GFP, and GFP::HCP-1 markers were transferred into transgenic strains by mating before analysis.

RNA-mediated interference (RNAi)

Double-stranded RNAs (dsRNAs) used in this study are listed in Table S2. For imaging, the dsRNA was injected into L4 worms and incubated for

38–43 h at 20°C. For double and triple RNAi, RNAs were mixed in equal ratios, with final concentrations of >0.7 mg/ml for each dsRNA.

Immunoblotting

For immunoblotting, worms from an NGM+OP50 agar plate were washed with M9 (22 mM KH_2PO_4, 42 mM Na_2HPO_4, 86 mM NaCl, and 1 mM $MgSO_4$•$7H_2O$) supplemented with 0.1% Triton X-100. After adding 100 µl of sterile glass beads to the ∼100 µl of pelleted worms and 50 µl of 4× sample buffer (40% glycerol, 240 mM Tris-HCl, pH 6.8, 8% SDS, 0.04% bromophenol blue, and 5% β-mercaptoethanol), samples were boiled and vortexed.

For immunoblotting after RNAi, L4 worms were injected with dsRNA and incubated for 40–42 h at 20°C. Worms were transferred into 500 µl of M9 and washed with 1 ml of M9 + 0.1% Triton X-100. 4× sample buffer was added and worms were lysed in an ultrasonic water bath for 10 min at 70°C; the final sample was comprised of 1 worm/µl. Samples were loaded onto 8% SDS gels, transferred to nitrocellulose, probed with 1 µg/ml affinity-purified anti–BUB-1 (rabbit; antigen was BUB-1 [aa 287–661]; Desai et al., 2003) and anti-KNL-1 (rabbit; antigen was KNL-1 [aa 8–256]; Desai et al., 2003), anti-BUB-3 (rabbit; antigen was BUB-3 [aa 189–329]; Essex et al., 2009), anti-SGO-1(rabbit; antigen was SGO-1 [aa 128–308]; generated in this study), or anti–α-tubulin (mouse monoclonal DM1-α; Sigma-Aldrich) antibodies.

Imaging and quantification

For imaging of one- and two-cell embryos, hermaphrodite adult worms were dissected into M9 buffer (22 mM KH_2PO_4, 42 mM Na_2HPO_4, 86 mM NaCl, and 1 mM $MgSO_4$•$7H_2O$), and embryos were transferred to 2% agarose pads positioned on a microscope slide and covered with an 18 × 18 nm coverslip.

Imaging of strains expressing GFP::H2B;γ-tubulin::GFP was performed on a deconvolution microscope (DeltaVision; Applied Precision/GE Healthcare) controlled by a softWoRx workstation (DeltaVision; Applied Precision/GE Healthcare) equipped with a charge-coupled device camera (CoolSNAP; Roper Scientific) with 5 × 2 µm z stacks, 2 × 2 binning, and a 60× 1.3 NA U-Plan-Apochromat objective lens (Olympus) at 10-s intervals and 100-ms exposure at 18°C. Acquired sequences were processed and analyzed using ImageJ (Fiji) and MetaMorph software (Molecular Devices). Pole tracking was performed by clicking on the center of each spindle pole and measuring the distance between them from NEBD onwards. NEBD was scored as the frame where free histone signal in the nucleus equilibrates with the cytoplasm, which is just before abrupt chromosome movement starts. Anaphase onset was scored as the first frame with visible separation of sister chromatids. Lagging chromatin was scored as visible threads of GFP::H2b signal between separating chromatid masses.

For all other strains, images were acquired on a spinning disc confocal system (Revolution XD Confocal System; Andor Technology) controlled by iQ software (Andor Technology) and a spinning disk confocal scanner unit (CSU-10; Yokogawa Electric Corporation) mounted on an inverted microscope (TE2000-E; Nikon) equipped with 100× or 60× 1.4 NA Plan-Apochromat lenses, and outfitted with an electron multiplication back-thinned charged-coupled device camera (iXon; Andor Technology) at 20°C.

To monitor BUB-1::GFP localization in the KNL-1::mCh mutants, a 5 × 2-µm z series, with 1 × 1 binning, was acquired every 20 s, with 200-ms and 300-ms exposure times for GFP and mCherry, respectively. For the separase sensor assay, mCh::H2B was monitored by acquiring 5 × 2 µm z-series, with 2 × 2 binning, every 20 s with 200-ms exposure time from NEBD to chromosome alignment. Then images for mCh::H2B and the GFP::Sensor were acquired as a 5 × 2-µm z series every 5 s with 200-ms exposure for GFP and for mCherry. To monitor GFP::HCP-1 localization, a 5 × 2-µm z series, with 1 × 1 binning, was acquired every 20 s, with 50-ms exposure for GFP and 300-ms exposure for mCherry. To monitor GFP::BUB-3 localization, a 5 × 2-µm z series, with 1 × 1 binning, was acquired every 20 s, with 200-ms exposure for GFP and 200-ms exposure for mCherry.

To quantify fluorescence, sequences were analyzed using ImageJ (Fiji). Z stacks were projected, a rectangular box was drawn around the entire chromosome set for each frame, and the integrated intensity in the box was recorded. Then the box was expanded by 5 pixels on each side, and the integrated intensity was measured. The signal and area difference between the expanded box and the original box were used to calculate the average background signal per pixel. The integrated chromosomal GFP intensity in the original box was then calculated by subtracting the background signal.

All p-values were calculated using unpaired *t* tests in GraphPad Prism (GraphPad Software).

Online supplemental material

Fig. S1 shows two additional examples of *bub-1(RNAi)* and characterization of the *bub-3(ok3437)* mutant. Fig. S2 shows the checkpoint signaling defect of KNL-1(Δ85-505) and the lack of an effect of the separase sensor on fertility, viability, or NEBD–anaphase onset duration. Fig. S3 shows characterization of the *bub-1(ok3383)* mutant, BUB-1 kinase domain variants, and the *sgo-1(tm2443)* mutant. Table S1 lists *C. elegans* strains used in this study and Table S2 lists oligos used to generate dsRNAs. Online supplemental material is available at http://www.jcb.org/cgi/content/full/jcb.201412035/DC1.

We thank Soni Lacefield for communicating unpublished work and Oegema/Desai laboratory members for useful discussions.

This work was supported by a National Institutes of Health grant (GM074215) to A. Desai. P. Lara-Gonzalez is a Pew Latin American Fellow, C. De Groot received support from the Deutsche Forschungsgemeinschaft, and M.W. Moyle was supported by Cancer Cell Biology (NIH-NCI-T32-CA067754) and UCSD Genetics (T32 GM008666) training grants. A. Desai and K. Oegema received salary and other support from Ludwig Cancer Research.

The authors declare no competing financial interests.

Submitted: 8 December 2014
Accepted: 20 April 2015

References

Bollen, M., D.W. Gerlich, and B. Lesage. 2009. Mitotic phosphatases: from entry guards to exit guides. *Trends Cell Biol.* 19:531–541. http://dx.doi.org/10.1016/j.tcb.2009.06.005

Chang, L., and D. Barford. 2014. Insights into the anaphase-promoting complex: a molecular machine that regulates mitosis. *Curr. Opin. Struct. Biol.* 29:1–9. http://dx.doi.org/10.1016/j.sbi.2014.08.003

Cheeseman, I.M., and A. Desai. 2008. Molecular architecture of the kinetochore-microtubule interface. *Nat. Rev. Mol. Cell Biol.* 9:33–46. http://dx.doi.org/10.1038/nrm2310

Cheeseman, I.M., I. MacLeod, J.R. Yates III, K. Oegema, and A. Desai. 2005. The CENP-F-like proteins HCP-1 and HCP-2 target CLASP to kinetochores to mediate chromosome segregation. *Curr. Biol.* 15:771–777. http://dx.doi.org/10.1016/j.cub.2005.03.018

Desai, A., S. Rybina, T. Müller-Reichert, A. Shevchenko, A. Shevchenko, A. Hyman, and K. Oegema. 2003. KNL-1 directs assembly of the microtubule-binding interface of the kinetochore in *C. elegans*. *Genes Dev.* 17:2421–2435. http://dx.doi.org/10.1101/gad.1126303

Di Fiore, B., N.E. Davey, A. Hagting, D. Izawa, J. Mansfeld, T.J. Gibson, and J. Pines. 2015. The ABBA motif binds APC/C activators and is shared by APC/C substrates and regulators. *Dev. Cell*. 32:358–372. http://dx.doi.org/10.1016/j.devcel.2015.01.003

Encalada, S.E., J. Willis, R. Lyczak, and B. Bowerman. 2005. A spindle checkpoint functions during mitosis in the early *Caenorhabditis elegans* embryo. *Mol. Biol. Cell*. 16:1056–1070. http://dx.doi.org/10.1091/mbc.E04-08-0712

Espeut, J., D.K. Cheerambathur, L. Krenning, K. Oegema, and A. Desai. 2012. Microtubule binding by KNL-1 contributes to spindle checkpoint silencing at the kinetochore. *J. Cell Biol.* 196:469–482. http://dx.doi.org/10.1083/jcb.201111107

Essex, A., A. Dammermann, L. Lewellyn, K. Oegema, and A. Desai. 2009. Systematic analysis in *Caenorhabditis elegans* reveals that the spindle checkpoint is composed of two largely independent branches. *Mol. Biol. Cell*. 20:1252–1267. http://dx.doi.org/10.1091/mbc.E08-10-1047

Félix, M.A., J.C. Labbé, M. Dorée, T. Hunt, and E. Karsenti. 1990. Triggering of cyclin degradation in interphase extracts of amphibian eggs by cdc2 kinase. *Nature*. 346:379–382. http://dx.doi.org/10.1038/346379a0

Fernius, J., and K.G. Hardwick. 2007. Bub1 kinase targets Sgo1 to ensure efficient chromosome biorientation in budding yeast mitosis. *PLoS Genet.* 3:e213. http://dx.doi.org/10.1371/journal.pgen.0030213

Frøkjær-Jensen, C., M.W. Davis, C.E. Hopkins, B.J. Newman, J.M. Thummel, S.-P. Olesen, M. Grunnet, and E.M. Jorgensen. 2008. Single-copy insertion of transgenes in *Caenorhabditis elegans*. *Nat. Genet.* 40:1375–1383. http://dx.doi.org/10.1038/ng.248

Gharbi-Ayachi, A., J.-C. Labbé, A. Burgess, S. Vigneron, J.-M. Strub, E. Brioudes, A. Van-Dorsselaer, A. Castro, and T. Lorca. 2010. The substrate of Greatwall kinase, Arpp19, controls mitosis by inhibiting protein phosphatase 2A. *Science*. 330:1673–1677. http://dx.doi.org/10.1126/science.1197048

Gillett, E.S., C.W. Espelin, and P.K. Sorger. 2004. Spindle checkpoint proteins and chromosome-microtubule attachment in budding yeast. *J. Cell Biol.* 164:535–546. http://dx.doi.org/10.1083/jcb.200308100

Grallert, A., E. Boke, A. Hagting, B. Hodgson, Y. Connolly, J.R. Griffiths, D.L. Smith, J. Pines, and I.M. Hagan. 2015. A PP1-PP2A phosphatase relay controls mitotic progression. *Nature*. 517:94–98. http://dx.doi.org/10.1038/nature14019

Hoyt, M.A., L. Totis, and B.T. Roberts. 1991. *S. cerevisiae* genes required for cell cycle arrest in response to loss of microtubule function. *Cell*. 66:507–517. http://dx.doi.org/10.1016/0092-8674(81)90014-3

Hunt, T. 2013. On the regulation of protein phosphatase 2A and its role in controlling entry into and exit from mitosis. *Adv. Biol. Regul*. 53:173–178. http://dx.doi.org/10.1016/j.jbior.2013.04.001

Jablonski, S.A., G.K. Chan, C.A. Cooke, W.C. Earnshaw, and T.J. Yen. 1998. The hBUB1 and hBUBR1 kinases sequentially assemble onto kinetochores during prophase with hBUBR1 concentrating at the kinetochore plates in mitosis. *Chromosoma*. 107:386–396. http://dx.doi.org/10.1007/s004120050322

Johnson, V.L., M.I.F. Scott, S.V. Holt, D. Hussein, and S.S. Taylor. 2004. Bub1 is required for kinetochore localization of BubR1, Cenp-E, Cenp-F and Mad2, and chromosome congression. *J. Cell Sci.* 117:1577–1589. http://dx.doi.org/10.1242/jcs.01006

Kang, J., M. Yang, B. Li, W. Qi, C. Zhang, K.M. Shokat, D.R. Tomchick, M. Machius, and H. Yu. 2008. Structure and substrate recruitment of the human spindle checkpoint kinase Bub1. *Mol. Cell*. 32:394–405. http://dx.doi.org/10.1016/j.molcel.2008.09.017

Kawashima, S.A., Y. Yamagishi, T. Honda, K. Ishiguro, and Y. Watanabe. 2010. Phosphorylation of H2A by Bub1 prevents chromosomal instability through localizing shugoshin. *Science*. 327:172–177. http://dx.doi.org/10.1126/science.1180189

Klebig, C., D. Korinth, and P. Meraldi. 2009. Bub1 regulates chromosome segregation in a kinetochore-independent manner. *J. Cell Biol.* 185:841–858.

Kraft, C., F. Herzog, C. Gieffers, K. Mechtler, A. Hagting, J. Pines, and J.-M. Peters. 2003. Mitotic regulation of the human anaphase-promoting complex by phosphorylation. *EMBO J.* 22:6598–6609. http://dx.doi.org/10.1093/emboj/cdg627

Kramer, E.R., N. Scheuringer, A.V. Podtelejnikov, M. Mann, and J.M. Peters. 2000. Mitotic regulation of the APC activator proteins CDC20 and CDH1. *Mol. Biol. Cell*. 11:1555–1569. http://dx.doi.org/10.1091/mbc.11.5.1555

Labit, H., K. Fujimitsu, N.S. Bayin, T. Takaki, J. Gannon, and H. Yamano. 2012. Dephosphorylation of Cdc20 is required for its C-box-dependent activation of the APC/C. *EMBO J.* 31:3351–3362. http://dx.doi.org/10.1038/emboj.2012.168

Lara-Gonzalez, P., F.G. Westhorpe, and S.S. Taylor. 2012. The spindle assembly checkpoint. *Curr. Biol.* 22:R966–R980. http://dx.doi.org/10.1016/j.cub.2012.10.006

Larsen, N.A., J. Al-Bassam, R.R. Wei, and S.C. Harrison. 2007. Structural analysis of Bub3 interactions in the mitotic spindle checkpoint. *Proc. Natl. Acad. Sci. USA*. 104:1201–1206. http://dx.doi.org/10.1073/pnas.0610358104

Liu, J., S. Vasudevan, and E.T. Kipreos. 2004. CUL-2 and ZYG-11 promote meiotic anaphase II and the proper placement of the anterior-posterior axis in *C. elegans*. *Development*. 131:3513–3525. http://dx.doi.org/10.1242/dev.01245

London, N., and S. Biggins. 2014. Mad1 kinetochore recruitment by Mps1-mediated phosphorylation of Bub1 signals the spindle checkpoint. *Genes Dev.* 28:140–152. http://dx.doi.org/10.1101/gad.233700.113

London, N., S. Ceto, J.A. Ranish, and S. Biggins. 2012. Phosphoregulation of Spc105 by Mps1 and PP1 regulates Bub1 localization to kinetochores. *Curr. Biol.* 22:900–906. http://dx.doi.org/10.1016/j.cub.2012.03.052

Meraldi, P., and P.K. Sorger. 2005. A dual role for Bub1 in the spindle checkpoint and chromosome congression. *EMBO J.* 24:1621–1633. http://dx.doi.org/10.1038/sj.emboj.7600641

Mochida, S., S.L. Maslen, M. Skehel, and T. Hunt. 2010. Greatwall phosphorylates an inhibitor of protein phosphatase 2A that is essential for mitosis. *Science*. 330:1670–1673. http://dx.doi.org/10.1126/science.1195689

Monen, J., N. Hattersley, A. Muroyama, D. Stevens, K. Oegema, and A. Desai. 2015. Separase cleaves the N-tail of the CENP-A related protein CPAR-1 at the meiosis I metaphase-anaphase transition in *C. elegans*. *PLoS ONE*. 10:e0125382. http://dx.doi.org/10.1371/journal.pone.0125382

Moore, L.L., M. Morrison, and M.B. Roth. 1999. HCP-1, a protein involved in chromosome segregation, is localized to the centromere of mitotic chromosomes in *Caenorhabditis elegans*. *J. Cell Biol.* 147:471–480. http://dx.doi.org/10.1083/jcb.147.3.471

Moyle, M.W., T. Kim, N. Hattersley, J. Espeut, D.K. Cheerambathur, K. Oegema, and A. Desai. 2014. A Bub1-Mad1 interaction targets the Mad1-Mad2 complex to unattached kinetochores to initiate the spindle checkpoint. *J. Cell Biol.* 204:647–657. http://dx.doi.org/10.1083/jcb.201311015

Murray, A.W., and M.W. Kirschner. 1989. Cyclin synthesis drives the early embryonic cell cycle. *Nature*. 339:275–280. http://dx.doi.org/10.1038/339275a0

Musacchio, A., and E.D. Salmon. 2007. The spindle-assembly checkpoint in space and time. *Nat. Rev. Mol. Cell Biol.* 8:379–393. http://dx.doi.org/10.1038/nrm2163

Nasmyth, K., and C.H. Haering. 2009. Cohesin: its roles and mechanisms. *Annu. Rev. Genet.* 43:525–558. http://dx.doi.org/10.1146/annurev-genet-102108-134233

Oegema, K., A. Desai, S. Rybina, M. Kirkham, and A.A. Hyman. 2001. Functional analysis of kinetochore assembly in *Caenorhabditis elegans*. *J. Cell Biol.* 153:1209–1226. http://dx.doi.org/10.1083/jcb.153.6.1209

Onn, I., J.M. Heidinger-Pauli, V. Guacci, E. Unal, and D.E. Koshland. 2008. Sister chromatid cohesion: a simple concept with a complex reality. *Annu. Rev. Cell Dev. Biol.* 24:105–129. http://dx.doi.org/10.1146/annurev.cellbio.24.110707.175350

Peters, J.M., R.W. King, C. Höög, and M.W. Kirschner. 1996. Identification of BIME as a subunit of the anaphase-promoting complex. *Science*. 274:1199–1201. http://dx.doi.org/10.1126/science.274.5290.1199

Pines, J. 2011. Cubism and the cell cycle: the many faces of the APC/C. *Nat. Rev. Mol. Cell Biol.* 12:427–438. http://dx.doi.org/10.1038/nrm3132

Portier, N., A. Audhya, P.S. Maddox, R.A. Green, A. Dammermann, A. Desai, and K. Oegema. 2007. A microtubule-independent role for centrosomes and aurora a in nuclear envelope breakdown. *Dev. Cell*. 12:515–529. http://dx.doi.org/10.1016/j.devcel.2007.01.019

Primorac, I., and A. Musacchio. 2013. Panta rhei: the APC/C at steady state. *J. Cell Biol.* 201:177–189. http://dx.doi.org/10.1083/jcb.201301130

Primorac, I., J.R. Weir, E. Chiroli, F. Gross, I. Hoffmann, S. van Gerwen, A. Ciliberto, and A. Musacchio. 2013. Bub3 reads phosphorylated MELT repeats to promote spindle assembly checkpoint signaling. *eLife*. 2:e01030. http://dx.doi.org/10.7554/eLife.01030

Ricke, R.M., K.B. Jeganathan, L. Malureanu, A.M. Harrison, and J.M. van Deursen. 2012. Bub1 kinase activity drives error correction and mitotic checkpoint control but not tumor suppression. *J. Cell Biol.* 199:931–949. http://dx.doi.org/10.1083/jcb.201205115

Roberts, B.T., K.A. Farr, and M.A. Hoyt. 1994. The *Saccharomyces cerevisiae* checkpoint gene BUB1 encodes a novel protein kinase. *Mol. Cell. Biol.* 14:8282–8291.

Sacristan, C., and G.J.P.L. Kops. 2014. Joined at the hip: kinetochores, microtubules, and spindle assembly checkpoint signaling. *Trends Cell Biol.*

Santaguida, S., and A. Musacchio. 2009. The life and miracles of kinetochores. *EMBO J.* 28:2511–2531. http://dx.doi.org/10.1038/emboj.2009.173

Sharp-Baker, H., and R.H. Chen. 2001. Spindle checkpoint protein Bub1 is required for kinetochore localization of Mad1, Mad2, Bub3, and CENP-E, independently of its kinase activity. *J. Cell Biol.* 153:1239–1250. http://dx.doi.org/10.1083/jcb.153.6.1239

Shepperd, L.A., J.C. Meadows, A.M. Sochaj, T.C. Lancaster, J. Zou, G.J. Buttrick, J. Rappsilber, K.G. Hardwick, and J.B.A. Millar. 2012. Phosphodependent recruitment of Bub1 and Bub3 to Spc7/KNL1 by Mph1 kinase maintains the spindle checkpoint. *Curr. Biol.* 22:891–899. http://dx.doi.org/10.1016/j.cub.2012.03.051

Sullivan, M., and D.O. Morgan. 2007. Finishing mitosis, one step at a time. *Nat. Rev. Mol. Cell Biol.* 8:894–903. http://dx.doi.org/10.1038/nrm2276

Sullivan, M., N.C.D. Hornig, T. Porstmann, and F. Uhlmann. 2004. Studies on substrate recognition by the budding yeast separase. *J. Biol. Chem.* 279:1191–1196. http://dx.doi.org/10.1074/jbc.M309761200

Tang, Z., H. Shu, D. Oncel, S. Chen, and H. Yu. 2004. Phosphorylation of Cdc20 by Bub1 provides a catalytic mechanism for APC/C inhibition by the spindle checkpoint. *Mol. Cell*. 16:387–397. http://dx.doi.org/10.1016/j.molcel.2004.09.031

Taylor, S.S., E. Ha, and F. McKeon. 1998. The human homologue of Bub3 is required for kinetochore localization of Bub1 and a Mad3/Bub1-related protein kinase. *J. Cell Biol.* 142:1–11. http://dx.doi.org/10.1083/jcb.142.1.1

Taylor, S.S., D. Hussein, Y. Wang, S. Elderkin, and C.J. Morrow. 2001. Kinetochore localisation and phosphorylation of the mitotic checkpoint components Bub1 and BubR1 are differentially regulated by spindle events in human cells. *J. Cell Sci.* 114:4385–4395.

Uhlmann, F., D. Wernic, M.A. Poupart, E.V. Koonin, and K. Nasmyth. 2000. Cleavage of cohesin by the CD clan protease separin triggers anaphase in yeast. *Cell*. 103:375–386. http://dx.doi.org/10.1016/S0092-8674(00)00130-6

Vanoosthuyse, V., R. Valsdottir, J.-P. Javerzat, and K.G. Hardwick. 2004. Kinetochore targeting of fission yeast Mad and Bub proteins is essential for spindle checkpoint function but not for all chromosome segregation roles of Bub1p. *Mol. Cell. Biol.* 24:9786–9801. http://dx.doi.org/10.1128/MCB.24.22.9786-9801.2004

Wang, X., J.R. Babu, J.M. Harden, S.A. Jablonski, M.H. Gazi, W.L. Lingle, P.C. de Groen, T.J. Yen, and J.M. van Deursen. 2001. The mitotic checkpoint protein hBUB3 and the mRNA export factor hRAE1 interact with

GLE2p-binding sequence (GLEBS)-containing proteins. *J. Biol. Chem.* 276:26559–26567. http://dx.doi.org/10.1074/jbc.M101083200

Wang, R., Z. Kaul, C. Ambardekar, T.G. Yamamoto, K. Kavdia, K. Kodali, A.A. High, and R. Kitagawa. 2013. HECT-E3 ligase ETC-1 regulates securin and cyclin B1 cytoplasmic abundance to promote timely anaphase during meiosis in C. elegans. *Development*. 140:2149–2159. http://dx.doi.org/10.1242/dev.090688

Warren, C.D., D.M. Brady, R.C. Johnston, J.S. Hanna, K.G. Hardwick, and F.A. Spencer. 2002. Distinct chromosome segregation roles for spindle checkpoint proteins. *Mol. Biol. Cell*. 13:3029–3041. http://dx.doi.org/10.1091/mbc.E02-04-0203

Wieser, S., and J. Pines. 2015. The biochemistry of mitosis. *Cold Spring Harb. Perspect. Biol.* 7:a015776. http://dx.doi.org/10.1101/cshperspect.a015776

Yamagishi, Y., T. Honda, Y. Tanno, and Y. Watanabe. 2010. Two histone marks establish the inner centromere and chromosome bi-orientation. *Science*. 330:239–243. http://dx.doi.org/10.1126/science.1194498

Yamagishi, Y., C.-H. Yang, Y. Tanno, and Y. Watanabe. 2012. MPS1/Mph1 phosphorylates the kinetochore protein KNL1/Spc7 to recruit SAC components. *Nat. Cell Biol.* 14:746–752. http://dx.doi.org/10.1038/ncb2515

Yudkovsky, Y., M. Shteinberg, T. Listovsky, M. Brandeis, and A. Hershko. 2000. Phosphorylation of Cdc20/fizzy negatively regulates the mammalian cyclosome/APC in the mitotic checkpoint. *Biochem. Biophys. Res. Commun.* 271:299–304. http://dx.doi.org/10.1006/bbrc.2000.2622